Nuclear Physics **A420** (1984) 297–319
© North-Holland Publishing Company

STATIC NUCLEAR PROPERTIES AND THE PARAMETRISATION OF SKYRME FORCES

F. TONDEUR

Physique Nucléaire Théorique and Institut d'Astrophysique, Université Libre de Bruxelles, CP 229
and
Institut Supérieur Industriel de Bruxelles, Bruxelles, Belgium

M. BRACK

Institut für Theoretische Physik, Universität Regensburg, Regensburg, Germany

M. FARINE

Faculty of Sciences, The Lebanese University, Mansourieh, El-Metn, Lebanon
and
Laboratoire de Physique Nucléaire, Département de Physique, Université de Montréal, Montréal, PQ, Canada

and

J.M. PEARSON

Laboratoire de Physique Nucléaire, Département de Physique, Université de Montréal, Montréal, PQ, Canada

Received 24 November 1983

Abstract: We present a systematic study of the dependence of static nuclear properties on the parameters of the effective interaction used in the Hartree–Fock (HF) and extended-Thomas–Fermi (ETF) models. For this purpose, a set of trial Skyrme forces, which are constrained by a fit to nuclear radii and binding energies, is developed. This leaves six free parameters: the spin-orbit strength, the nuclear-matter compression modulus, the isoscalar and isovector contributions to the effective masses, the value of the exchange parameter x_3 (governing the surface-symmetry properties) and the coefficient of the "gradient-symmetry" term $|\nabla\rho_n - \nabla\rho_p|^2$ in the energy-density functional. The influence of these parameters on various properties is studied: droplet-model parameters, quality of the fit to experimental masses, extrapolation of masses, fit to charge radii, charge distributions and neutron-skin thicknesses, semiclassical fission barriers, and Landau parameters. Indications are given of the directions which could be followed in order to improve the fit to experimental data. Several correlations remaining in the results suggest that a larger number of degrees of freedom obtained by additional terms could be useful.

1. Introduction

With the use of Skyrme forces, the Hartree–Fock (HF) method showed ten years ago [1]) its ability to reach an overall agreement with experiment for nuclear ground-state properties. Although good results have also been obtained with more realistic interactions [2–4]), the Skyrme forces still remain a very useful tool in view of their simplicity. However, it soon became apparent that the original forces of Vautherin

and Brink [1]) as well as the well-known Skyrme–Orsay forces [5]) could be improved, and that a more detailed agreement with experiment, including dynamical properties, was possible. New forces have been proposed with a lower compression modulus K [ref. [6–9])], also giving good predictions for the giant resonances [7]) and the fission barriers for heavy nuclei [8,9]). It seems now that it might be possible to obtain simultaneously a fair agreement with experiment for masses, radii, giant resonances and fission barriers, although none of these recent forces fully reaches this goal. The ability of Skyrme forces to reproduce spectroscopic properties, expressed e.g. by Landau parameters, has also been examined [10,11]), showing an advantage of the density-dependent version of the force over its original three-body expression [12]). New forces taking spectroscopic constraints into account have also been proposed [13]) but their application to deformed nuclei or fission barriers has not yet been undertaken. All these works represent very interesting steps towards a good "multipurpose force", which however still has to be built.

The same forces have been used more recently in the extended-Thomas–Fermi (ETF) model [9,14]) which gives a description of the average trends of static nuclear properties and provides a link between HF and phenomenological models often used in nuclear physics, such as the droplet model (DM).

The HF and ETF calculations have, in particular, revealed some deficiences of the DM [9,15,16]), and can be expected to replace it in many fields where unknown nuclear properties must be predicted. Consequently the need increases for an accurate description of several nuclear properties with HF and ETF models. This can only be obtained if a sufficient flexibility is given to the force to allow a fit to a large amount of data. The standard Orsay forces [5]), which are here written in their density-dependent form [11])

$$V = t_0(1+x_0P_\sigma)\delta + \tfrac{1}{2}t_1(1+x_1P_\sigma)(\boldsymbol{k}'^2\delta + \delta\boldsymbol{k}^2) + t_2(1+x_2P_\sigma)\boldsymbol{k}'\cdot\delta\boldsymbol{k} + \tfrac{1}{6}t_3(1+x_3P_\sigma)\rho^\alpha\delta + iW_0\boldsymbol{\sigma}\cdot\boldsymbol{k}'\times\delta\boldsymbol{k}, \quad (1)$$

take $x_1 = x_2 = 0$, $x_3 = 1$ and $\alpha = 1$, and thus include six free parameters. Five constraints being given by a rough fit to masses, radii and spin-orbit splittings, only one degree of freedom is left, implying strong correlations between the parameters, e.g. between K and the effective mass m^*.

A separate fit of m^* and K is possible when $\alpha \neq 1$ is allowed [6]). With $x_3 \neq 1$ [ref. [6])], the surface-symmetry properties can also be varied separately [but this degree of freedom is still poorly explored, e.g. in refs. [7,8]) where $x_3 = 0$]. As a consequence of the limited freedom of many proposed forces, it is quite difficult to fit them to a large set of data or to extend them to new fields. It is also difficult to understand in detail the relations between the calculated nuclear properties and the parameters of the force due to the remaining correlations between those parameters.

More general forces are thus needed. A first generalisation, allowing for x_1 and $x_2 \neq 0$, has been considered in order to improve the spectroscopic properties of the force [11]) with, however, a bad fit to ground-state binding energies. Interesting results

have also been obtained with new terms included in the force [12,13,17]), but a systematic study of the contributions of those terms to the various nuclear properties is not yet available.

At this point of the development of Skyrme forces, we believe that a more systematic approach has become necessary. To improve the forces, we must know how each parameter of the interaction influences the various physical results of the model. This might indeed allow us to know which terms in the force are actually necessary to reproduce a given set of data or which experimental data are the most useful to fit the parameters of the force, and also to estimate the accuracy of the predictions of unknown nuclear properties.

The aim of the present paper is to give a preliminary discussion of these questions, restricted to a particular class of interaction:

(a) including all terms given in eq. (1);

(b) giving a reasonable fit to ground-state nuclear masses and charge radii in the HF+BCS model.

Further work is planned, to include other terms in the force. The development of forces which do not reproduce the ground-state properties [or reproduce them badly, like SkM [7]) or SG [11]) forces] could also be of interest for purely spectroscopic purposes, but will not be considered here.

The type of force we consider has ten free parameters. A rough fit to masses and radii (including data for neutron-rich nuclei) gives four constraints, which correspond more or less to the four terms of the old liquid-drop mass formula: volume, surface, symmetry and Coulomb energies, the latter being fixed by the fit to radii. Starting from one force, we can thus follow six independent directions in the parameter space. Sect. 2 indicates how those directions have been chosen, and gives a set of forces showing how the parameters vary along each direction. The corresponding variations of the droplet-model parameters are given in sect. 3, whereas sect. 4 examines the application of the forces to binding-energy calculations. Sect. 5 studies the density distributions obtained with the different forces, and sect. 6 shows the variations of the average (semiclassical) part of fission barrier heights. Finally, we discuss the Landau parameters and pairing properties corresponding to the forces in sect. 7, before summarising and discussing our results in sect. 8.

We want to emphasize that the purpose of the present paper is not to add another set to the already disordered multitude of Skyrme forces existing in the literature, but to provide the necessary tool for a more systematic approach. Though it could happen that one of the forces we present would be suitable for use in specific problems, their main interest is not in the qualities of the forces themselves but in their differences.

2. The interactions

With the force given by (1), the binding energy of a time-reversal symmetric spherical nucleus can be written in the HF approximation as the integral of a

hamiltonian density:

$$\mathcal{H}=\frac{\hbar^2}{2m_n}\tau_n+\frac{\hbar^2}{2m_p}\tau_p+\tfrac{1}{2}t_0\Big[(1+\tfrac{1}{2}x_0)\rho^2-(x_0+\tfrac{1}{2})\sum_q\rho_q^2\Big]$$
$$+\tfrac{1}{4}t_1\Big[(1+\tfrac{1}{2}x_1)(\rho\tau+\tfrac{3}{4}(\nabla\rho)^2)-(x_1+\tfrac{1}{2})\sum_q(\rho_q\tau_q+\tfrac{3}{4}(\nabla\rho_q)^2)-\tfrac{1}{4}x_1\boldsymbol{J}^2+\tfrac{1}{4}\sum_q\boldsymbol{J}_q^2\Big]$$
$$+\tfrac{1}{4}t_2\Big[(1+\tfrac{1}{2}x_2)(\rho\tau-\tfrac{1}{4}(\nabla\rho)^2)+(x_2+\tfrac{1}{2})\sum_q(\rho_q\tau_q-\tfrac{1}{4}(\nabla\rho_q)^2)-\tfrac{1}{4}x_2\boldsymbol{J}^2-\tfrac{1}{4}\sum_q\boldsymbol{J}_q^2\Big]$$
$$+\tfrac{1}{12}t_3\Big[(1+\tfrac{1}{2}x_3)\rho^2-(x_3+\tfrac{1}{2})\sum\rho_q^2\Big]\rho^\alpha+\tfrac{1}{2}W_0\Big(\boldsymbol{J}\cdot\nabla\rho+\sum_q\boldsymbol{J}_q\cdot\nabla\rho_q\Big)\,, \tag{2}$$

where the densities ρ_q, τ_q and $\boldsymbol{J}_q$ are defined as usual [1]), the unlabeled densities being implicitly summed over q (=n or p).

Two groups of terms in (2) will play a particular role in the discussion. The first one concerns the terms including $(\nabla\rho)^2$ or $(\nabla\rho_q)^2$ which can be written in the following form:

$$\eta(\nabla\rho)^2+\zeta(\nabla\rho_n-\nabla\rho_p)^2\,, \tag{3}$$

where

$$\eta=\tfrac{1}{64}(9t_1-5t_2-4t_2x_2)\,, \tag{4}$$
$$\zeta=-\tfrac{1}{64}(3t_1+t_2+6t_1x_1+2t_2x_2)\,. \tag{5}$$

We shall refer to the first and second terms in (3) as to the "gradient" and "gradient symmetry" (GS) terms, respectively.

The second group of terms in (2) we want to consider are those including the kinetic densities τ_q, from which we define the usual effective mass m_q^*:

$$m_q^{*-1}=m_q^{-1}+\frac{\rho}{8\hbar^2}(3t_1+5t_2+4t_2x_2)$$
$$\pm\frac{\rho_n-\rho_p}{8\hbar^2}(t_2-t_1+2t_2x_2-2t_1x_1)\,, \tag{6}$$

where the plus sign holds for neutrons and the minus sign for protons. We shall refer to the first two terms in the right-hand side of (6) as to the isoscalar part of the effective mass (more precisely of the inverse effective mass), the last term being its isovector part.

We emphasize the fact that the $\boldsymbol{J}^2$ terms in (2), which are usually neglected in standard Skyrme codes, will be kept in the following calculations. We also notice that the HF code we use computes the Coulomb energy and single-particle potential from the folded charge density, not from the proton point density. The usual Coulomb exchange and diagonal part of c.m. corrections are included.

TABLE 1

Parameters of the forces (values are consistent with the use of MeV and fm as the units of energy and length)

	t_0	t_1	t_2	t_3	x_0	x_1	x_2	x_3	W_0	α	V_0
T1	−1794.0	298	−298	12 812	0.154	−0.5	−0.5	0.089	110	$\frac{1}{3}$	−210
T2	−1791.6	300	−300	12 792	0.154	−0.5	−0.5	0.089	120	$\frac{1}{3}$	−210
T3	−1791.8	298.5	−99.5	12 794	0.138	−1	1	0.075	126	$\frac{1}{3}$	−210
T4	−1808.8	303.4	−303.4	12 980	−0.177	−0.5	−0.5	−0.5	113	$\frac{1}{3}$	−210
T5	−2917.1	328.2	−328.2	18 584	−0.295	−0.5	−0.5	−0.5	114	$\frac{1}{6}$	−210
T6	−1794.2	294	−294	12 817	0.392	−0.5	−0.5	0.5	107	$\frac{1}{3}$	−210
T7	−1892.5	366.6	−21	11 983	0.334	−0.359	6.9	0.366	109	0.285	−235
T8	−1892.5	367	−228.76	11 983	0.448	−0.5	−0.5	0.695	109	0.285	−235
T9	−1891.4	377.4	−239.16	11 982	0.441	−0.5	−0.5	0.686	130	0.285	−235
T1*	−1800.5	296	−296	12 884	0.157	−0.5	−0.5	0.092	95	$\frac{1}{3}$	−210
T3	−1800.5	296	−98.67	12 884	0.142	−1	1	0.076	95	$\frac{1}{3}$	−210

To start with an effective interaction giving good fits to masses and radii, we first adjust a Skyrme force reproducing approximately the functional $\mathcal{H}$ used by one of us [18]) in HF calculations, and which has been shown to reproduce those quantities with a good accuracy. The resulting parameters are given in table 1 (force T1). This force, like the original functional, is characterised by an effective mass m^* equal to the bare nucleon mass, a realistic value of the compression modulus K of nuclear matter ($K = 236$ MeV) and no gradient-symmetry term ($\zeta = 0$). However, we note that there is no force exactly equivalent to the functional used in ref. [18]) because of the $\boldsymbol{J}^2$ terms in (2) not included in ref. [18]), and of a different form of the density dependence of the symmetry terms in $\mathcal{H}$ in nuclear matter. Another small difference is due to the different procedure followed when folding the proton density distribution. [We take here the usual gaussian folding with an rms radius of 0.8 fm for the proton; a lower value was taken in ref. [18]), which can simulate the neutron contribution to the charge density.]

As in ref. [19]), the pairing correlations are included in the BCS framework for non-magic nuclei, the pairing matrix elements being obtained with a δ-force of constant strength $V_0 = 210$ MeV · fm^3.

New forces are then built starting from T1 by varying separately the remaining free characteristic parameters, as described hereafter and as summarised in fig. 1.

(a) T2 is obtained from T1 by increasing the spin–orbit strength W_0 by 9%, while keeping constant effective masses ($m^* = m$) and density dependence power α (and thus, as will be shown hereafter, a constant K), as well as a constant ($\zeta = 0$) gradient-symmetry term and a constant x_3 (x_0). (The value of x_0 being strongly correlated with x_3, due to the fit to masses, we shall take x_3 as the free parameter in several cases, but will recall the corresponding influence on x_0 by the notation x_3 (x_0).) The other parameters are refitted to reproduce a good fit to a few masses (^{16}O, ^{56}Fe, ^{90}Zr, ^{118}Sn, ^{132}Sn, ^{138}Ba, ^{208}Pb) and to the rms charge radius of ^{208}Pb.

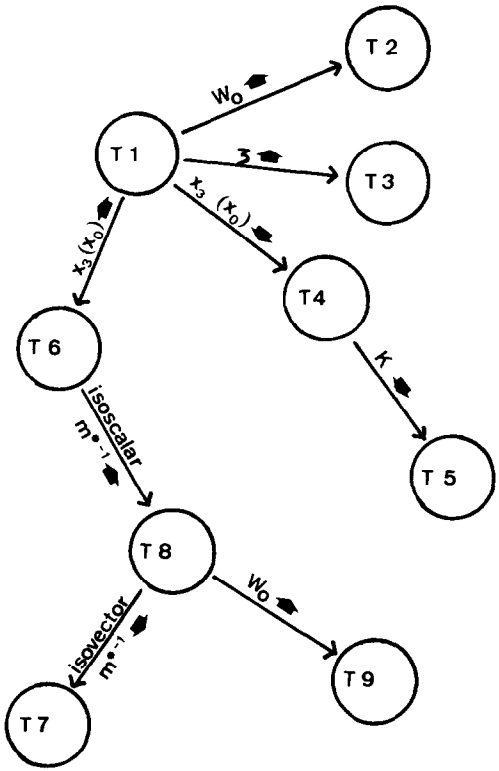

Fig. 1. Schematic view of the differences between the trial Skyrme forces. ζ represents the coefficient of the gradient-symmetry term (eq. (5)), whereas the two contributions to $(m^*)^{-1}$ are defined in eq. (6). See the text for a detailed description.

(b) T3 is obtained from T1 by introducing a positive gradient-symmetry (GS) term in $\mathcal{H}$, with constant m^* and α. Under the $m^* = m$ constraint, the variation of the gradient-symmetry term is accompanied by an increase of the $\boldsymbol{J}^2$ terms, which must be compensated by some increase of W_0. The latter is fitted in T3 in such a way as to keep the same average value as T1 for the spin-orbit splittings in the last filled and first empty shells of ^{208}Pb. Other parameters have been refitted to keep the good fit to masses and radius of ^{208}Pb as in T2.

In order to separate the contributions of the gradient-symmetry and $\boldsymbol{J}^2$ terms in variation T1 → T3, two forces T1* and T3* have also been fitted in which the $\boldsymbol{J}^2$ terms are neglected.

(c) T4 is obtained from T1 by decreasing x_3 (x_0), with constant m^*, α and GS term (=0), other parameters being refitted to keep the good fit to the masses, and to the ^{208}Pb radius and average of spin–orbit splittings in ^{208}Pb.

(d) T5 is obtained from T4 by decreasing the density-dependence power α, with constant m^*, x_3 and GS term, other parameters being refitted as previously.

(e) A major consequence of the low x_3 (x_0) values in T4 and T5 is the increase of the neutron-skin thickness of heavy nuclei, which is then found to be too large

compared with experiment. In T6, we try to improve the agreement with experiment for this quantity by increasing x_3 (x_0). The variations T1 → T4 and T1 → T6 are thus redundant, following opposite directions in the parameter space.

(f) We now release the constraint $m^* = m$; m^*/m being lowered to $\frac{5}{6}$ in symmetric nuclear matter at saturation in T7. This quantity is however, still kept equal to 1 in pure neutron or pure proton matter, by the proper fit of the isovector part of m^*. From T6 to T7, we keep constant K, and neutron-skin thickness in ^{208}Pb, other parameters being refitted as previously. The constant neutron skin is taken here as an indicator of constant surface-symmetry properties. The variation of x_3 (x_0) from T6 to T7 is quite small, showing that a rough correlation is still present between x_3 (x_0) and these properties, at least for reasonable values of m^*. Because of the increase of the single-particle level spacings when $m^* < m$, the pairing strength has to be increased too, $V_0 = 235$ MeV · fm^3 being used in forces T7, T8 and T9. The large value of x_2 in T7 is not worrying, the real physical parameter being the product t_2x_2, which is still small.

(g) T8 is obtained by putting $m^*/m = \frac{5}{6}$ in neutron matter too at the nuclear-matter saturation density, thus cancelling the isovector contribution to $(m^*)^{-1}$. Other fits are the same as in T7. T8 can also be derived from T6 by increasing the isoscalar part of $(m^*)^{-1}$, and T7 from T8 by varying its isovector part.

(h) The major consequence of the lower m^* introduced in T7 and T8 is a worse fit to masses. This fit is however improved if W_0 is multiplied by $\frac{6}{5}$, to increase the spin–orbit splittings by the same factor as the average level spacings. This is done in T9. The change from T8 and T9 is of the same type as from T1 to T2. We emphasize once more that none of these interactions is considered by us to be more than a tool for studying the dependence of various physical results on the force. Although they already include several improvements with respect to many of the available forces, this aspect will not be examined here, because there is no reason to think that one of them can be definitive for any particular purpose.

The six directions in the parameter space which can be explored with those forces are finally related to the spin–orbit strength W_0, the gradient-symmetry term, the neutron-skin thickness, the compression modulus of nuclear matter, and the isoscalar and isovector effective masses, under the constraint of a reasonable fit to masses and charge radii. Previous studies with the Skyrme forces do not allow such a wide exploration of the parameter space. In particular, the spin–orbit, gradient-symmetry and isovector $(m^*)^{-1}$ degrees of freedom have never been varied separately while maintaining a good fit to the masses and radii.

3. Droplet-model parameters

Several trends of nuclear properties can be quite easily understood if the DM parameters corresponding to the forces are known. These parameters are the coefficients of the DM expansion of the volume energy

$$E_v = A(a_v + \tfrac{1}{2}K\varepsilon^2 + J\delta^2 - L\varepsilon\delta^2) \tag{7}$$

and of the surface energy

$$E_s = A^{2/3}[a_s(1+2\varepsilon) + Q\theta^2], \tag{8}$$

where

$$\varepsilon = (\rho_\infty - \rho_c)/3\rho_\infty, \tag{9}$$

$$\delta = (\rho_{cn} - \rho_{cp})/\rho_c, \tag{10}$$

ρ_∞ being the nuclear-matter saturation density, ρ_c the average core density, and θ the DM dimensionless neutron-skin thickness,

$$\theta = \left(\frac{N\rho_\infty}{\rho_{cn}}\right)^{1/3} - \left(\frac{Z\rho_\infty}{\rho_{cp}}\right)^{1/3}. \tag{11}$$

The volume parameters a_v, K, J and L, as well as ρ_∞, can be easily obtained from the functional (2) by using the kinetic-energy density of a Fermi gas:

$$\tau_q = \tfrac{3}{5}(3\pi^2)^{2/3}\rho_q^{5/3}. \tag{12}$$

Several approaches are possible for evaluating the DM surface coefficients (a_s, Q). One is to perform a HF calculation for semi-infinite nuclear matter from which the surface coefficients can be extracted [20,21]). This model is free from any assumption about the nuclear surface, and is the obvious extension of the HF model for finite nuclei, thus ensuring the adequacy of the forces for such a model. However, the numerical accuracy of the results ($\approx$0.2 MeV for a_s) is of the same order as the variations from one force to another.

A second method uses the extended-Thomas–Fermi approach [9,22–24]) which can be compared to the DM. This is usually done by using the semiclassical gradient expansion for $\tau[\rho]$ [refs. [24,25])] and by varying the density profiles (for finite nuclei or for semi-infinite nuclear matter). The accuracy of ETF results is thus dependent on the quality of the semiclassical functional $\tau[\rho]$ and on the variational subspace chosen for the density profiles. However, the good numerical accuracy of ETF calculations allows one to compare in detail the results obtained with different forces.

Estimations of surface coefficients from HF binding energies obtained for finite nuclei have sometimes been made [52]). The accuracy of this approach is bad and will not be considered here.

We compare in table 2 the surface parameters of the various forces obtained by the ETF and HF methods. We notice that Q^{HF} is obtained from the analysis of surface-symmetry energies in semi-infinite matter. This parameter can also be estimated from the neutron-skin thickness, with a worse accuracy. The ETF coefficients are obtained for semi-infinite matter with a generalised Fermi density profile [9]):

$$\rho_q = \rho_{\infty q}\left[1 + \exp\left(\frac{z - Z_q}{a_q}\right)\right]^{-\gamma}, \tag{13}$$

TABLE 2

Droplet-model coefficients and other characteristic parameters

	T1	T2	T3	T4	T5	T6	T7	T8	T9
k_F (fm^{-1})	1.336	1.336	1.336	1.330	1.344	1.336	1.335	1.335	1.334
ρ_∞ (fm^{-3})	0.1610	0.1610	0.1611	0.1590	0.1640	0.1609	0.1606	0.1607	0.1608
a_v (MeV)	−15.98	−15.94	−15.96	−15.95	−15.99	−15.96	−15.94	−15.94	−15.88
K (MeV)	236.1	235.7	235.9	235.5	201.7	235.9	235.6	235.7	234.9
J (MeV)	32.02	32.00	31.50	35.45	37.00	29.97	29.52	29.92	29.76
L (MeV)	56.2	56.2	55.3	94.1	98.5	30.9	31.1	33.7	33.7
a_s^{HF} (MeV)	18.3	18.1	17.9	18.2	18.2	18.3	18.3	18.2	17.9
a_s^{ETF} (MeV)	17.99	17.77	17.66	17.90	17.97	17.95	17.90	17.90	17.61
a_s^{ETF} ($\gamma=1$)	18.28	18.04	17.93	18.19	18.34	18.23	18.19	18.19	17.88
Q^{HF} (MeV)	33	33	34	26	25	40	41	41	43
Q^{ETF} (MeV)	36.5	36.4	38.5	27.9	26.9	46.8	46.7	46.1	45.1
a_c^{ETF} (MeV)	11.4	11.5	11.5	11.4	12.6	11.3	11.2	11.2	11.5
m^*/m ($\delta=0$)	1	1	1	1	1	1	$\frac{5}{6}$	$\frac{5}{6}$	$\frac{5}{6}$
m^*/m ($\delta=1$)	1	1	1	1	1	1	1	$\frac{5}{6}$	$\frac{5}{6}$

where q = n or p, and where z measures the distances perpendicular to the surface of semi-infinite matter.

Table 2 also displays the coefficients describing the volume properties, as well as the Fermi momentum k_F in nuclear matter at saturation. The curvature coefficient has been calculated in ETF by using the leptodermous expansion [9]). We also recall for convenience the values of m^*/m in symmetric nuclear matter ($\delta=0$) and in pure neutron or proton matter ($|\delta|=1$) at $\rho=\rho_\infty$.

Table 2 shows several noteworthy results, several of them already pointed out in other works. The first one is the correlation between ρ_∞ and K, already demonstrated for a wider class of forces by Blaizot *et al.* [26,27]). Our results show that ρ_∞ is indeed almost insensitive to all free parameters, except K, for a set of forces reproducing the same rms charge radius for ^{208}Pb. The value of $\Delta K/\Delta k_F \approx 2450$ MeV · fm is in good agreement with the trend suggested in ref. [26]) (≈2000 MeV · fm). A more detailed analysis of HF results shows however that the explanations invoked by Blaizot for this correlation are not sufficient. The first one is that a lower K should favour a larger compression (dilatation) in all nuclei which have a compressed (dilated) core with respect to infinite nuclear matter. In the fits we present, ρ_∞ is of course mainly determined by the fit to the charge radius of ^{208}Pb which is dilated. We can thus expect a larger dilatation with T5, which must be compensated by a higher ρ_∞ in order to keep a constant radius. However, we expect then in lighter compressed nuclei a cumulative effect of a larger compression and a large ρ_∞, leading to a decrease of the radii when K is decreased. The results instead show for ^{40}Ca and ^{56}Fe that the core density is only slightly influenced by K, the significant increase of ρ_∞ from T4 to T5 being nearly cancelled by a larger dilatation, as in ^{208}Pb, although the former nuclei have compressed cores. In ^{16}O, the dilatation effect is even dominant and larger than the increase of ρ_∞.

The second reason given by Blaizot for the $\rho_\infty - K$ correlation is a consequence of the increase of the surface diffuseness (and thus of the rms radius) when K is decreased. This variation of the surface diffuseness is also found in our results (see sect. 5). A constant rms radius in ^{208}Pb can then be obtained by increasing ρ_∞. This effect is not negligible, but quite small. Indeed, the average core density in ^{208}Pb, as well as its central density, show only a 0.4% increase from T4 to T5, in contrast to the 3% increase of ρ_∞. Clearly, ^{208}Pb and most other nuclei we have considered are more dilated (or less compressed) with respect to nuclear matter when K is lower, as with T5.

Other results, including those examined in sect. 5, confirm the existence of a dilatation effect at low K, which will be discussed elsewhere in more detail [41]).

We now consider the asymmetry coefficients J, L and Q. A systematic difference of $\approx 10\%$ is observed between HF and ETF values for Q, which can be due to the approximations of the ETF model, as stated before, but also to a small departure from the expansion (8) in HF results: in view of the limited numerical accuracy of E_s, it is not possible to obtain the value of Q corresponding to very small values of θ for which the expansion (8) is valid. Therefore, the accuracy of Q^{HF} is probably not much better than 2 MeV, and the agreement between ETF and HF can be considered as very satisfactory.

The major variations of J, L and Q are strongly correlated, as noticed in previous works [21,29]). A correlation between J and Q seems natural for forces giving a good fit to masses: any decrease of the volume-symmetry energy must be balanced by an increase of the surface-symmetry energy to keep the more or less constant total symmetry energy needed for the mass fit. However, the correlation between L and the two other parameters could be a characteristic of the type of forces we consider, i.e. forces which do not produce a true "surface-symmetry" term in the energy-density functional, e.g.

$$(\rho_n - \rho_p)^2 (\nabla \rho)^2 . \tag{14}$$

In this case indeed, the symmetry energy at the surface only comes from the symmetry energy of nuclear matter at the local density. As a consequence, a low (high) volume-symmetry energy (at $\rho \approx \rho_\infty$) together with a high (low) surface-symmetry energy (at $\rho < \rho_\infty$) means a small (large) variation of the symmetry energy with the density, i.e. a small (large) L.

We note that the GS term $\zeta(\nabla \rho_n - \nabla \rho_p)^2$ added in T3 does not play the role of a surface-symmetry term. It does not influence Q very much, and has large "volume" contributions coming from the density oscillations in the core.

As noticed before, x_3 (x_0) is also roughly correlated with Q, and thus with J and L. This correlation is very strong for a set of force with the same m^* (e.g. forces T1 to T6), but is particular to the forces examined here. Preliminary calculations which will be reported elsewhere indeed show that the addition of new terms in the force allows one to break the correlation between x_3 (x_0) and J, Q, L.

We finally consider the surface and curvature parameters in table 2. In view of their numerical accuracy (≈ 0.2 MeV), the HF values of a_s cannot be invoked to show the influence of the force. Their absolute value, which in principle should be better than the ETF values, is nearly constant (≈ 18.1 MeV) within this accuracy, this being of course due to the fit to the masses. The small variations of a_s^{HF} are however consistent with those obtained in ETF results, which are slightly smaller when calculated with an asymmetric Fermi shape ($\gamma \neq 1$). A part of the small difference ($\approx 2\%$) between a_s^{HF} and a_s^{ETF} can be attributed to the ETF approximation of the functional $\tau[\rho]$, which is known [9,14]) to slightly overbind finite nuclei in variational calculations. One should notice however that HF density profiles are not very asymmetric, due to the presence of the Friedel oscillations which are not included in ETF calculations. Taking a symmetric Fermi distribution ($\gamma = 1$) in ETF calculations could thus give a better approximation to HF and indeed leads to a very good agreement with HF for the value of a_s.

The only significant variations of a_s (observed in ETF values) are related to the variations of the spin–orbit strength W_0, e.g. between T8 and T9. On the other hand, the curvature coefficient a_c (equivalent to the a_3 of the DM) is only slightly sensitive to one parameter: the compression modulus K (varied from T4 to T5).

4. Binding energies

The differences between experimental and calculated binding energies for a few spherical (or nearly spherical) nuclei are given in table 3. It is not possible from such a small set of results to draw detailed conclusions about the mass fit. However, a general feature appears: the fit is worsened when m^* is lowered from m to $\frac{5}{6}m$.

TABLE 3

Differences between experimental and calculated binding energies (MeV)

	T1	T2	T3	T4	T5	T6	T7	T8	T9
^{16}O	+0.7	−1.4	+1.1	+0.8	+0.8	+0.3	−1.6	−1.5	+0.4
^{32}S	+2.1	−0.1	+1.8	+1.6	+0.9	+2.4	+4.8	+4.6	+0.7
^{40}Ca	−0.3	+1.2	+0.8	−0.3	−0.5	−1.1	−3.9	−3.9	+0.4
^{48}Ca	−0.1	−0.8	−1.6	−1.1	−0.5	+0.2	−1.3	−1.0	−1.1
^{56}Fe	+1.5	−0.5	+0.5	+1	+1.5	+1.6	+4.6	+3.4	+0.6
^{72}Ge	0	+0.2	−0.5	−0.3	−1.2	−0.3	−0.7	−1.0	+1.9
^{90}Zr	0	−0.6	−1.3	−0.3	0	0	−1.2	−1.1	−0.2
^{100}Ru	+0.4	−0.1	−0.6	+0.1	−0.8	+0.4	+1.9	+1.5	+2.1
^{110}Cd	+0.7	+0.4	−0.1	+0.5	−0.2	+0.5	+2.1	+1.6	+2.9
^{118}Sn	−0.2	−0.5	−0.9	−0.5	−0.9	−0.4	0	−0.3	+1.3
^{132}Sn	−1.0	−2.8	−1.6	−2.4	−1.8	+0.1	+1.6	+0.2	−2.7
^{138}Ba	−0.6	−1.3	−1.6	−1.0	−0.6	−0.3	+0.6	−0.2	−0.3
^{146}Gd	+0.3	+0.3	−0.7	+0.2	+0.2	0	+0.3	−0.2	+1.9
^{208}Pb	+0.4	+0.4	+0.4	+1.1	+0.5	0	+1.1	−0.1	0

It is indeed well known that the shell effects in masses are very sensitive to m^* and are reasonably well reproduced with $m^* \approx m$, as in mass formulae based on the Strutinsky method [30]). The effective mass is thus a crucial parameter if a specialised force for calculations of masses is needed. The high m^* giving a good fit is however in contradiction with the estimates based on the energies of deeply bound states or on the isoscalar quadrupole giant resonance. The value $m^* = m$ in fact simulates the result of correlations neglected in the HF + BCS model. Probably, using a force with $m^* < m$ and explicitly taking those correlations into account, one could also obtain a good fit to masses. The quite heavy numerical treatment needed in such an approach unfortunately prohibits presently its extension to a very large number of nuclei, e.g. for a systematic mass prediction. For large-scale extrapolations, $m^* \approx m$ thus seems to be a good approximation, and the comparison of the predictions obtained with the nine forces should thus be focussed on forces T1 to T6. Less crude approximations are currently examined, but are beyond the scope of the present work. To compare rapidly the mass extrapolations far from the known region, we present in table 4 the binding energies of ^{74}Cr, ^{266}Pb (which are neutron-rich) and $^{354}_{126}X_{228}$ (a nearly β-stable superheavy nucleus). We also give the value of the $N = 50$ gap in the single particle spectrum of ^{74}Cr, which has been shown [19]) to be greatly weakened in the neutron-rich region. The influence of the force on this gap can also be of interest as an example of extrapolation of the shell effects.

In ^{74}Cr and in ^{266}Pb, the main variation of the binding energy is found when x_3 (x_0) is varied (T4 → T1 → T6). Changing x_3 from $-\frac{1}{2}$ to $+\frac{1}{2}$ induces a 9.5 MeV variation of the energy of ^{74}Cr, and 14.5 MeV for ^{266}Pb. These differences are of course related to the large variations of J and Q from T4 to T6. This shows that, although reasonable fits to known masses can be obtained with quite different values of J and Q, a proper choice of these parameters is crucial for a good extrapolation.

Other parameters induce smaller but still significant variations of the binding energies of ^{74}Cr and ^{266}Pb. To show to what extent these variations are due to the shell effects, we also show for ^{266}Pb the ETF binding energies, which mostly confirm

TABLE 4

Binding energies of nuclei far from the known region (MeV)

	^{74}Cr	^{74}Cr (gap)	^{266}Pb^{HF}	^{266}Pb^{ETF}	$^{354}_{126}X_{228}$
T1	−566.1	2.08	−1807.1	−1777.2	−2360.4
T2	−567.7	2.33	−1805.8	−1775.6	−2357.9
T3	−567.1	2.06	−1810.4	−1784.3	−2362.9
T4	−571.8	2.04	−1816.0	−1787.1	−2358.2
T5	−572.2	1.65	−1820.7	−1790.5	−2356.9
T6	−562.3	2.06	−1801.4	−1771.2	−2361.7
T7	−561.6	2.09	−1806.3	−1778.8	−2363.5
T8	−562.0	2.32	−1802.4	−1772.3	−2360.4
T9	−564.9	2.83	−1803.3	−1772.0	−2357.9

the HF results, except in the case of T1 → T3. In T3, a positive value is given to the gradient-symmetry term, which is probably underestimated in ETF calculations, as explained in the next section. We thus conclude that the differences observed between the various HF predictions are mostly due to the average trends, not to local shell effects, so the conclusions drawn for two particular nuclei can reveal general features.

The extrapolation to $^{354}_{126}X_{228}$, with 146 nucleons added to ^{208}Pb (the heaviest nucleus used in the fit of the forces) does not lead to strongly divergent predictions. Variations of 2–3 MeV are there typical from one force to another. Extrapolations along the β-stability line can thus be much more accurate than extrapolations towards the drip lines, and a proper fit of the force could probably lead to quite reliable mass predictions in this region.

The possibility of accurate extrapolations towards the drip lines is more doubtful, and would need the estimation of the correct value of J within ±0.5 MeV and a corresponding value of Q within ±2 MeV. (For the forces with $m^* = m$ considered here, this is equivalent to an accuracy of ±0.1 for x_3.) Looking at the quantities which are the most sensitive to J and Q, we find a required accuracy of ±0.01 fm for the neutron skin thickness of ^{208}Pb, while the experimental error bar is ≈0.05 fm (see sect. 5). As for fission barriers, an accuracy of ≈0.3 MeV would be required for actinide nuclei, which is probably beyond the accuracy of the HF + BCS calculation. We thus believe that, even if good fits can be achieved, the properties of neutron-rich nuclei will always be predicted with a rather large error bar. The estimation of the error, based for example on the present set of forces, could be necessary for example in several astrophysical problems. (Information on J and Q can also be extracted from the giant dipole resonance, but the interpretation is a bit confused by the dependence on m^*. This problem is currently being examined.)

In many questions, mass differences are also needed, which are very sensitive to the shell effects. As shown for the $N = 50$ magic gap in ^{74}Cr, these effects are sensitive to the effective mass and spin–orbit strength, but also to the compression modulus K (T4 → T5) which influences the single-particle spectra through its influence on the surface diffuseness [18]).

5. Density distributions

Table 5 gives a few examples of rms charge radii obtained with the nine forces. We point out that all forces have been fitted to the radius of ^{208}Pb. We are therefore mainly interested in the variations of the radii of light and medium nuclei, the heavy ones being quite insensitive to the force due to the constraint on ^{208}Pb. Two results are particularly noteworthy. The first one is that the difference Δr_c between the charge radii of ^{40}Ca and ^{48}Ca can be modified by changing several parameters such as the effective mass (a decrease of m^* increases Δr_c: T6 → T7 → T8), and to a lesser

TABLE 5

(a) RMS radii, equivalent sharp radii and 90%–10% surface thickness of the HF charge distribution for a few nuclei (in fm)

	T1	T2	T3	T4	T5	T6	T7	T8	T9
^{16}O	2.75	2.75	2.75	2.76	2.79	2.75	2.74	2.74	2.76
	2.90	2.90	2.90	2.91	2.93	2.90	2.90	2.90	2.91
	2.27	2.28	2.27	2.28	2.34	2.27	2.25	2.25	2.28
^{40}Ca	3.48	3.48	3.49	3.49	3.51	3.48	3.47	3.47	3.48
	3.91	3.92	3.92	3.92	3.92	3.91	3.91	3.91	3.91
	2.56	2.57	2.57	2.57	2.66	2.56	2.56	2.56	2.58
^{48}Ca	3.51	3.51	3.50	3.51	3.52	3.51	3.52	3.52	3.52
	4.02	4.03	4.02	4.02	4.01	4.03	4.03	4.03	4.03
	2.43	2.42	2.41	2.43	2.51	2.44	2.44	2.45	2.45
^{90}Zr	4.28	4.28	4.28	4.29	4.30	4.29	4.28	4.29	4.29
	5.10	5.10	5.10	5.10	5.08	5.10	5.07	5.08	5.10
	2.45	2.45	2.43	2.45	2.57	2.45	2.59	2.54	2.50
^{208}Pb	5.50	5.50	5.50	5.50	5.50	5.50	5.50	5.50	5.50
	6.76	6.76	6.76	6.76	6.74	6.77	6.77	6.77	6.76
	2.44	2.44	2.44	2.44	2.52	2.44	2.47	2.46	2.46
(b) Density oscillation in ^{208}Pb (fm^{-3})									
$\delta\rho_c$ (^{208}Pb)	0.0052	0.0052	0.0040	0.0050	0.0048	0.0056	0.0049	0.0056	0.0056
(c) Surface thickness of semi-infinite nuclear matter (fm)									
HF	2.38	2.34	2.31	2.38	2.62	2.38	2.40	2.39	2.34
ETF	2.14	2.13	2.12	2.14	2.29	2.13	2.13	2.14	2.13

extent K and x_3 [as already noticed with Köhler's forces [6])]. The main variation however is found between T1 and T3.

By considering the forces T1* and T3* in which the $\boldsymbol{J}^2$ terms are neglected, it is found that the reduction of Δr_c does not come from the GS term in T3, but mainly from the $\boldsymbol{J}^2$ terms and the simultaneous readjustment of W_0. As some further reduction of Δr_c (≈ -0.01 fm) can be obtained when the contribution of the neutrons to the charge density is included, the result obtained with T3 is quite satisfactory and shows that the $\boldsymbol{J}^2$ terms should not be neglected when a detailed fit of nuclear properties is wanted. [We notice that the good Δr_c obtained without $\boldsymbol{J}^2$ terms with SkM* [8]) could be worsened by correcting the overbinding of ^{48}Ca obtained with this force, which is probably accompanied by some reduction of the charge radius of this nucleus.]

A second result is that T5 gives significantly larger charge radii for light nuclei, e.g. ^{16}O and ^{40}Ca. This effect combines the dilatation at low K discussed in sect. 3 with an increase of the surface thickness, also shown in table 5. In view of the

weakness of the influence of other parameters, in the range considered here, quite high values of K ($K \approx 240$ MeV) seem necessary [31]) to reproduce the trends of the charge radii in HF with a Skyrme force. A definitive fit however can only be done after choosing the values of other parameters, and after including corrections in the charge radius neglected here [45]), in which ground-state correlations could play a role [46]).

To distinguish between the diffuseness and dilatation effects, we also show in table 5 the DM equivalent sharp radius and the 90%–10% surface thickness for the charge density defined as in refs. [25,32]). Although these quantities cannot be defined unambiguously for several nuclei like ^{40}Ca, the arbitrary definition we use is here sufficient because we only want to display variations from one force to another.

We notice in particular the dilatation of ^{16}O when K is lowered (T4 → T5) whereas ^{208}Pb, ^{90}Zr and ^{48}Ca are compressed (as well as nuclear matter) and ^{40}Ca unchanged. This is related to the discussion given in sect. 3 of a dilatation effect when the surface diffuseness is increased. This effect appears thus to be larger at low A.

The increase of the surface thickness can be noticed from T4 to T5. Other parameters have a smaller influence on it on the average, which is probably related to shell effects; it is indeed not found in ETF results and in semi-infinite matter HF results.

The correlation between K and the surface diffuseness can be understood in terms of the balance between the two main contributions to the surface energy: the binding energy of nuclear matter at $\rho < \rho_\infty$, which is lowered when K is low, and the gradient contribution to $\mathcal{H}$ which has thus to be higher when K is low, the total surface energy being more or less constrained by the fit to masses. A higher positive $(\nabla\rho)^2$ term in $\mathcal{H}$ obviously favours a lower gradient, i.e. a large diffuseness when K is low. The surface diffuseness could thus give good indications for a fit of K. For example, after including all usual corrections to the charge density [45]), the fit to the surface thickness of ^{208}Pb with $m^* = m$ is consistent with $K = 230$–250 MeV, in good agreement with the previous estimation based on the radii. Comparison with other forces suggest that the effective mass could influence the diffuseness when m^* is much lower than considered here; with $m^* = 0.61m$, Köhler [6]) indeed obtains a reasonable diffuseness in ^{208}Pb although his force has $K = 263$ MeV, thus extending the possible range of K towards higher values. Reasonable diffuseness and radii are also obtained with $K = 306$ MeV (force S5), but with an unrealistic $m^*/m = 0.38$ [ref. [5])].

These values of K are larger than the current estimations based on the energy of the giant monopole resonance. It should be recalled however that the GDR allows an estimate of the compressibility K_A of finite nuclei, from which K has to be extrapolated, with more or less crude assumptions on the variations of K_A with A, in particular on the value of the surface compressibility K_s. As pointed out in [49]), K_s is very sensitive to the compression mode of the GDR, and deviations from the scaling mode (for which $K_s \approx -K$) could lead to values of K significantly larger

than 220 ± 20 MeV given in ref. [50]). In this context, the indications given by density distributions are in favour of a slightly higher K. We also recall that the compressibility K influences the single-particle spectra, as noticed in sect. 4 for the $N = 50$ magic gap in ^{74}Cr. An earlier fit of K based on such data [12]) gives $K = 220$–250 MeV.

We point out that the dependence of the density distribution on K (k_F) is not universal: a class of forces is presented in ref. [28]) for which k_F can be varied with nearly no effect on the density distributions, even though the correlation with K is maintained. A further study of those forces is, however, necessary to understand why they give this result.

We now examine the question of density oscillations in the core of nuclei, taking ^{208}Pb as an example. Defining $\delta\rho_c$ as the difference between the central value of the charge density $\rho_c(0)$ and the first minimum of $\rho_c(r)$, we obtain the values displayed in table 5, which are on the average 2–3 times larger than the experimental result. An interesting point is that it is thus possible to reduce $\delta\rho_c$ by varying several parameters, mainly the coefficient of the GS term (T1 → T3)†. This is due to the fact that ρ_n and ρ_p vary out of phase in the core of ^{208}Pb, giving quite large oscillations of $\rho_n - \rho_p$, which are damped when a positive $|\nabla(\rho_n - \rho_p)|^2$ term is introduced in $\mathcal{H}$. This also explains why in HF calculations the GS term is not a pure surface term, although it contributes only to the surface when a pure Fermi distribution is used in ETF calculations. This suggests that ETF will not reproduce the average trends of HF when the GS term is large, especially if it is negative, and thus amplifies the density oscillations. However, the GS term cannot be too negative, because $\delta\rho_c$ soon becomes completely unrealistic, and even induces serious convergence problems in the HF code. This puts a constraint on the possible values of x_1 for a Skyrme force like (1). Except for forces giving a large isovector effective mass (i.e. $m^* > m$ in neutron matter), only negative or slightly positive values of x_1 can be accepted.

Apart from the trivial influence of ρ_∞, the two crucial parameters influencing the charge densities with the forces we have considered are K and x_1. They influence ρ_n in a similar way. On the other hand, we still have to examine which parameters determine the difference between ρ_n and ρ_p, and in particular the neutron-skin thickness, defined as the difference between rms radii of neutron and proton densities. This quantity is given in table 6 for a few nuclei. The largest variations are obtained for ^{208}Pb when x_3 (x_0) is varied (T4 → T1 → T6). They correspond to the large variations of the surface-stiffness parameter Q described in sect. 3. The good agreement between HF and ETF results for ^{208}Pb confirm the weakness of the shell effects in the neutron-skin thickness [33]).

The neutron-skin thickness is potentially the best source of information for the determination of Q and hence of J, the importance of which, for the extrapolation of masses near the drip lines, has been discussed in sect. 4. In the case of the forces examined here, this determination of Q will also serve to fix x_3 (x_0). The case of

† The neutron correction to ρ_c also reduces $\delta\rho_c$.

TABLE 6

Neutron-skin thickness (in fm)

	^{40}Ca	^{48}Ca	^{90}Zr	^{208}Pb		Semi-∞ ($\delta^2 = 0.02$)
	HF	HF	HF	HF	ETF	HF
T1	−0.05	0.18	0.06	0.19	0.18	0.27
T2	−0.04	0.17	0.06	0.19	0.19	0.26
T3	−0.04	0.18	0.06	0.19	0.19	0.24
T4	−0.05	0.21	0.09	0.25	0.24	0.37
T5	−0.05	0.22	0.09	0.26	0.26	0.38
T6	−0.05	0.16	0.05	0.15	0.15	0.21
T7	−0.05	0.16	0.06	0.15	0.15	0.20
T8	−0.05	0.16	0.06	0.15	0.15	0.21
T9	−0.05	0.15	0.05	0.15	0.15	0.20

^{208}Pb is particularly interesting, because of the stronger dependence of the neutron-skin thickness on the force, and to the effort made [35]) to obtain a rather reliable experimental result (0.14 ± 0.04 fm, which implies $J = 29 \pm 2$ MeV and $Q = 45 \pm 10$ MeV). This corresponds for the Skyrme forces considered here to $0 \leqslant x_3 \leqslant 1$. Other results e.g. for ^{90}Zr [ref. [36])] and ^{48}Ca [ref. [37])] are consistent with this, although the error bars are larger. The large values of J given by the DM mass fits thus seem to be excluded by the data concerning the neutron skin. However, these data are still controversial, in particular in view of the Gatchina [34]) results for ^{208}Pb (0.06 fm) and ^{90}Zr (0.15 fm) [an earlier analysis [39]) of the same results for ^{208}Pb even gives a slightly negative value!]. No force of the kind we examine can account for both results simultaneously, and indeed it seems that no available model of the neutron skin could, but drawing conclusions based only on the Los Alamos results could be premature. We notice however that $0 \leqslant x_3 \leqslant 1$ is consistent with the general prediction of the Brueckner theory [51]) that most of the density dependence of the effective force lies in the ^{3}S state and is always repulsive. On the other hand, the analysis of neutron-matter properties with Skyrme forces [38]) indicates that $x_3 \approx$ 0.3–0.6 is a rather appropriate value for this problem. This latter point could be of particular interest, because it allows for a determination of x_3 which does not depend on the possible inclusion of a surface-symmetry term like (14) in the energy-density functional $\mathcal{H}$. Neutron matter, however, is only known from theoretical models.

6. Fission barriers

All the results presented in the previous sections have been obtained for spherical shapes. It is of great importance also to test the ability of the forces to describe deformed shapes, and particularly the extremely deformed shapes encountered in fission. Detailed comparisons of HF fission barriers would however be very time-consuming. As a first step in a comparative study of fission barriers, we examine

here the average part of the barrier as given by the ETF model. We follow the method outlined in ref. [9]), which has been shown to be in good agreement with a Strutinsky-averaged HF calculation of the average part of the barrier [8]). The results we present hereafter are restricted to left/right and axially symmetric shapes, using the (c, h) parametrisation [40]) and pure Fermi shapes with constant diffuseness for the density distributions. Moreover, we restrict ourselves to the $h = 0$ path, which is known to give a good approximation to the liquid-drop fission path, and neglect the diffuseness corrections for the Coulomb energy. In view of those restrictions, we shall not try to give indications on how to fit the parameters of the force to fission-barrier heights, but only point out those parameters which have a crucial influence on the barriers. The values we give for ^{240}Pu should not be compared to liquid-drop results obtained for symmetric shapes ($\approx$3.8 MeV) without being corrected by a Coulomb diffuseness correction, a correction for $h \neq 0$, a correction for density distributions not restricted to Fermi shapes, and a correction for variations of the diffuseness with (c, h), the total correction being approximately -2.5 ± 0.5 MeV. When considering the results as giving the average trend of the HF barriers, one should also not forget that HF also contains a smooth spurious part because of the spurious rotational energy, which is not taken into account in ETF calculations.

The average barrier heights obtained for ^{240}Pu are given in table 7. They show that the two crucial parameters are W_0 and x_3 (x_0). It has been checked in the case T1 $\rightarrow$ T3 that the lowering of the barrier is due to the increase of W_0, the $\boldsymbol{J}^2$ terms and the GS term giving a slight increase of the barrier height. We notice that neither the variation of K, nor those of m^*, lead to significant changes in the barrier height.

The role of W_0 is of course related to its influence on the surface coefficient, shown in sect. 3. On the other hand, the influence of x_3 (x_0) is nothing else than the well-known influence of the surface-symmetry energy on the fission barrier, related to the variation of the DM parameters J and Q described in sect. 3.

As fission barriers are known with a better accuracy than the neutron skins, it could be interesting to use them for the fit of $Q(J)$ or equivalently, for the forces we consider, the fit of x_3 (x_0). As shown by our results, this can only done if the spin–orbit contributions are also known with a good accuracy. Until now, these terms have been very poorly handled in Skyrme-force fits, the $\boldsymbol{J}^2$ terms being neglected and W_0 being fitted very roughly. A fit of W_0 on spin–orbit splittings of

TABLE 7

ETF fission barrier of ^{240}Pu (MeV) (corrections not included can be estimated to -2.5 ± 0.5 MeV)

T1	7.5	T5	5.3
T2	6.8	T6	8.8
T3	6.8	T7	8.7
T4	5.7	T8	8.6

spin-saturated nuclei like ^{16}O gives [42]) $W_0 \approx 130$ MeV, a quite high value compared with our forces, thus favouring a low barrier. The agreement with experimental splittings for other nuclei however cannot be achieved without taking $\boldsymbol{J}^2$ terms into account [42]).

On the other hand, the values of Q or x_3 (x_0) should of course be fitted on microscopic asymmetric fission-barriers heights, and would depend on the strength of the shell effects (influenced by m^* and by the pairing strength) and on the inclusion of zero-point motion and spurious rotational-energy corrections. These corrections could be essential to obtain a simultaneous description of fission barriers and neutron skins.

We would like to notice that the interesting results already obtained with the force SkM* [8,9]), with $W_0 = 130$ MeV $\cdot$ fm^5 and $x_3 = 0$, agree quite well with the trends we present here, but this force overestimates the binding of neutron-rich nuclei. The ≈ 8 MeV overbinding of ^{132}Sn can correspond to an underestimation of the asymmetry coefficient J by ≈ 2 MeV. A new fit of J implies a readjustment of other liquid-drop parameters, and probably a decrease of the volume coefficient to ≈ -15.9 MeV and a slight increase of the surface coefficient (by ≈ 0.5 MeV in a rough estimation), with significant effects (2–3 MeV) on the fission barriers. The fit of a Skyrme force giving good fission barriers is thus still an open problem.

We finally notice that the correlation between x_3 (x_0) and the fission barriers, like the correlation between x_3 (x_0) and J, Q, L, is probably particular to the forces we consider; J and Q are the parameters which can be extracted from empirical fits, and their relations with the parameters of the force can vary according to the form of the interaction. The calculation of the DM parameters made in sect. 3 is thus an essential step in the study of the force, because it allows one to use the simple concepts of macroscopic models in the analysis of ETF of HF results.

7. Spectroscopic properties

In this paper, we are mainly concerned with ground-state properties, but even in this context it is necessary to consider spectroscopic properties at least to the extent of ensuring that the forces give the right ground state. The importance of this was first realized with the discovery [43]) that the original S2 force [1]) gives the 2^- state of ^{16}O below the lowest 0^+. A first approach to this problem consists in requiring that infinite matter be spin and spin-isospin stable. This can be expressed in terms of the Landau parameters of the Landau-Migdal theory of Fermi liquids [44]), in particular by requiring $G_0 > -1$ and $G_0' > -1$ [ref. [10])].

Table 8 shows the values of the four parameters F_0, F_0', G_0 and G_0', the expressions of which have been given by Giai and Sagawa [11]). All our forces except T3 satisfy the required conditions. This suggests that it might be difficult with the type of forces considered here to reconcile the spin stability ($G_0 > -1$) with a sufficient damping of the density oscillations.

TABLE 8
Landau parameters

	F_0	F'_0	G_0	G'_0
T1	0.06	1.60	−0.40	0.16
T3	0.06	1.55	−1.23	0.45
T4	0.07	1.90	−0.70	0.16
T5	−0.10	1.96	−0.88	0.05
T6	0.06	1.36	−0.22	0.18
T7	−0.11	1.00	−0.72	0.49
T8	−0.11	1.02	0.01	0.24

We also want to examine briefly another general spectroscopic feature of the effective interaction which can be of interest for ground-state properties: its pairing properties. There is no fundamental reason why the HF effective interaction should also work as a pairing interaction, although some interactions can be successfully used for both the mean field and the pair field [4]). Nevertheless, it is interesting to see to what extent our interactions can generate reasonable pairing.

Rather than making a systematic study in finite nuclei, we shall restrict the discussion to the case of infinite matter, as done for the Landau parameters. The interaction then reduces to

$$[t_0(1-x_0)+t_1(1-x_1)k_F^2+\tfrac{1}{6}t_3(1-x_3)\rho^\alpha]\delta(r)=V_0\delta(r) \tag{15}$$

for a pair of time-reversed states at the Fermi surface coupled to $S=0$ and $T=1$. All our nine forces have $V_0>0$, i.e. they give rise to anti-pairing rather than to pairing. Although surface effects will tend to lower the positive terms in (15), a reasonable value of V_0 (−200 to −250 MeV · fm^3 as suggested by the strength of the δ pairing force used in our HB+BCS calculations, see table 1) cannot be obtained with the rather low values of x_1 we have considered.

These poor pairing properties are to be contrasted with those of ref. [11]). However, these latter interactions developed specifically to good pairing characteristics and Landau parameters turn out to give poor mass fits, overbinding by several tens of MeV.

There is however no contradiction between a good fit to masses and good pairing properties. The finite-range Gogny force [4]), as well as the generalised Skyrme force